Nanostructural Characterization of Catfish Skin Gelatin Using Atomic Force Microscopy

HONGSHUN YANG, YIFEN WANG, JOE M. REGENSTEIN, AND DAVID B. ROUSE

ABSTRACT: To determine the nanostructure of gelatin from catfish (*Ictalurus punctatus*) skin, atomic force microscopy (AFM) was used to study gelatin aggregates. The gelatin was extracted at an optimized acid concentration after alkaline processing. First, the AFM imaging parameters were optimized to obtain high-quality images. Then height mode with a 2-dimensional plane, 3-dimensional topographical images, and error signal mode images, which removed slow variations in surface topography but highlighted the edges of sample features, were used to analyze the structure of particles. The results describe fish gelatin at a nanoscale level for the first time and are compared with AFM images of mammalian gelatins. Both annular pores with diameters averaging 118 nm and spherical aggregates with an average diameter of 267 nm were seen in the AFM images of fish gelatin. From the AFM images, we propose that the structures formed were determined by whether the solution penetrated into the gelatin molecules evenly or not during hydrolysis. A scheme for the formation of annular pores and spherical aggregates is proposed.

Keywords: atomic force microscopy (AFM), catfish, fish skins, gelatin, nanostructure, nanotechnology

Introduction

Gelatin has a wide range of applications in the food, pharmaceutical, and photographic industries. Most of the available gelatins are obtained from the hydrolysis of mammalian collagen. However, gelatin from fish skins has been attracting more interest in recent years because of safety, economic, religious, and environmental considerations (Cho and others 2006). Understanding and then improving the physical properties of fish gelatin is important for increasing its utilization. A number of studies discuss the physical properties of fish gelatin (Choi and Regenstein 2000; Yoshimura and others 2000; Gómez-Guillén and others 2002; Jamilah and Harvinder 2002; Cho and others 2006; Zhou and others 2006; Yang and others 2007a). The physical properties of gelatin are determined by its structure, which depends not only on the protein sequence, but also on the relative contents of various collagen breakdown components and their state of aggregation. In essence, gelatin is a water-soluble polypeptide derived from insoluble collagen, usually after acid or alkaline processing. The resulting gelatin depends on how this hydrolysis is performed, and the biological source material and its "quality" at the time of processing. However, gelatin is not as well defined structurally as other synthetic polymers (Benmouna and Johannsmann 2004). Only schematic structures of gelatin have been reported by Lin and others (2002).

Current instrumentation commonly used to show gelatin's intrinsic properties including determining the main components, the physical properties, and its microstructure are GC/HPLC (Jamilah and Harvinder 2002), rheometer (Jamilah and Harvinder 2002), spectrometer (Cho and others 2006), SEM/TEM (DiOrio and others 2005; Saxena and others 2005), electrophoretic analysis (Gómez-Guillén and others 2002; Zhou and others 2006), differential scanning calorimetry (Badii and Howell 2006), and FT-IR spectroscopy (Badii and Howell 2006). However, it is difficult to study the molecular structure of gelatin due to its high heterogeneity. Except with SEM/TEM, most other techniques give a sample-wide average for the gelatin, which does not reflect structural variability. On the other hand, the complicated pretreatment of samples for SEM/TEM sometimes obscures the sample's native structure (Yang and others 2007b).

Nanotechnology is currently receiving a great deal of attention in many areas of food science, including food protein gels (Foegeding 2006; Yang and others 2007b). Atomic force microscopy (AFM), as one of the tools for observing nanoscale processes, can directly image individual macromolecules and polymers. AFM has been successfully applied to the study of polysaccharides (Vardhanabhuti and Ikeda 2006; Yang and others 2006b) and proteins (Ikeda and Morris 2002; Ikeda 2003) in foods. As for application of AFM to collagen and gelatin, only high-purity laboratory-prepared mammalian samples were studied (Haugstad and Gladfelter 1993, 1994; Radmacher and others 1995; Chen and others 1998; Mackie and others 1998; Yao and others 1999; Lin and others 2002; Uricanu and others 2003; Benmouna and Johannsmann 2004; Usha and others 2004; Mohanty and Bohidar 2005; Saxena and others 2005). However, to the best of our knowledge, there have been no AFM studies of food-grade gelatin or gelatin from fish skins. Gelatin from catfish skins was chosen in this study because it is one of the most important farm-raised fishes in the United States and its skin accounts for about 6% of the initial fish weight. Thus, efforts are underway to improve the availability and utilization of catfish gelatin.

The objectives of this study were to determine the nanostructure of food-grade fish gelatin and to establish any relationships between the nanostructure and physical properties. To fulfill the main objectives, the AFM had to be optimized for fish gelatin, specifically the selection of the cantilever, tip, and imaging environments; and based on the parameter optimization, the nanostructure of catfish gelatin was determined and related to gel strength; and finally the

MS 20070430 Submitted 6/7/2007, Accepted 7/1/2007. *Authors Yang and Wang are with Biosystems Engineering Dept., Auburn Univ., 200 Tom E. Corley Building, Auburn, AL 36849-5417, U.S.A. Author Regenstein is with Dept. of Food Science, Cornell Univ., Ithaca, NY 14853-7201, U.S.A. Author Rouse is with Dept. of Fisheries and Allied Aquacultures, Auburn Univ., Auburn, AL 36849-5417, U.S.A. Author Yang is also with College of Food Science and Technology, Henan Univ. of Technology, Zhengzhou, Henan, 450052, P.R. China. Direct inquiries to author Wang (E-mail: wangyif@auburn.edu).*

© 2007 Institute of Food Technologists
doi: 10.1111/j.1750-3841.2007.00480.x
Further reproduction without permission is prohibited

results were compared to other studies on mammalian gelatins. In this study, the unmodified structure of gelatin under commercially relevant conditions was studied.

Materials and Methods

Gelatin preparation

The gelatin preparation used was optimized using the procedure of Yang and others (2007a). Frozen catfish skins were obtained courtesy of Harvest Select Inc. (Uniontown, Ala., U.S.A.). The frozen skins were stored at –18 °C with a maximum storage time of less than 2 mo before use. All reagents used in this study were analytical grade. The frozen skins were thawed at 4 °C for about 20 h, then cut into small pieces (about 2 to 3 cm squares) and washed with tap water (1:6 w/v) at 4 °C for 10 min. Washing was repeated 3 times. The cleaned fish skins were drained using 4 layers of cheesecloth for 5 min, and the cheesecloth containing the skins was then squeezed by hand to remove most of the liquid. Cleaned skins were put into a flask and treated with 0.20 M NaOH (1:6 w/v) for 84 min. Then, the samples were drained including the hand-squeezing step using the cheesecloth and rinsed with tap water (1:6 w/v). The above procedure was repeated 2 times, and then the samples were treated with 0.115 M acetic acid (1:6 w/v) for 60 min, drained using the cheesecloth and rinsed with tap water (1:6 w/v) 3 times. All of the solutions used in the above steps were kept at 4 °C. After the above pretreatment, deionized water (1:4 w/v) was added to the flasks. Parafilm (Structure Probe Inc/SPT Supplies, West Chester, Pa., U.S.A.) and aluminum foils were then used to cover the flasks and the samples were kept in a 55 °C water bath (Model 86; Precision Scientific Co., Chicago, Ill., U.S.A.) for 180 min. After that, the gelatin solutions were filtered through 4 layers of cheesecloth, and then the solution was lyophilized (Labconco Corp., Kansas City, Mo., U.S.A.).

Determination of gel strength

The lyophilized gelatin was dissolved at 6.67% (w/w) in distilled water. The mixture was allowed to stand until the gelatin was completely swollen, then heated in a 65 °C water bath (Model 2095-2; Forma Scientific Inc., Marietta, Ohio, U.S.A.), with stirring, until the gelatin was fully dissolved (approximately 30 min). Approximately 1 mL of the solution was saved in a refrigerator for later AFM determination. The other solution was then put into small plastic bottles (cylindrical-shaped solution bottles [Wheaton Industries Inc., Millville, N.J., U.S.A.] that are flat-bottomed with an average 31-mm internal dia × 25-mm height, with the largest diameter being 33 mm and the smallest 29 mm). After being matured at 10 °C for 17 ± 1 h, the gel was removed from the bottle using a thin blade knife, and the gel strength was determined using the TA.XTPlus Texture Analyzer (Texture Technologies Corp., Scarsdale, N.Y., U.S.A./Stable Micro Systems, Godalming, Surrey, U.K.) with a 12.5-mm-dia flat plastic plunger pressing 4 mm into the gelatin gel using a 5-kg load cell at a speed of 1 mm/s. The sample was assumed to have a temperature of 10 °C since it was measured immediately after being removed from 10 °C refrigeration. The maximum value of the force with units of "g" can be considered as the "bloom" strength since the measurement was made at 10 °C (Wainewright 1977).

AFM determination

The fish gelatin solution was taken from the refrigeration and equilibrated to room temperature (approximately 120 min). Heated in hot water (just above the melting temperature) for melting the gelatin, the melted solutions were then disrupted to disaggregate any gels remaining from the lower-temperature storage and to create a homogeneous mixture using a Vortex mixer (Fisher Scientific, Pittsburgh, Pa., U.S.A.). The solution was then diluted to about 10 to 40 μg/mL and deposited onto a piece of freshly cleaved mica sheets (about 1.0 × 1.0 cm^2) (Muscovite Mica; Electron Microscopy Sciences, Hatfield, Pa., U.S.A.), which was made by detaching the upper layer of the multilayer mica structure with adhesive tape. A small volume (about 20 μL) of the solution was pipetted rapidly (taking about 5 s) onto the mica surface to avoid possible conglomeration of gelatin. The mica surface was then air-dried before AFM imaging. To avoid the influence of dust from the laboratory on the sample imaging, each sample was freshly prepared just before the AFM viewing to minimize possible contamination of the sample surface by the surrounding air. The concentration of gelatin solution can be adjusted to optimize the images that can be obtained.

The nanostructure characterization was performed using a Nano-R2™ AFM (Pacific Nanotechnology Inc., Santa Clara, Calif., U.S.A.) in noncontact mode. The microscope was equipped with a Z scanner operating at ambient temperature. Figure 1 shows the schematic image of the AFM imaging process. Detailed information is available in a previous report by Yang and others (2007b). This AFM model has only 2 modes: the contact mode and the noncontact mode. The noncontact mode in this AFM is similar to the commonly used tapping mode found with other AFM equipments. The term "tapping mode" was registered as a trademark by another company. However, we use "tapping mode" to describe this format in the text as this is the term commonly used in the literature. The mica, along with the sample, was attached to a 15-mm-dia AFM specimen disc (TED Pella Inc., Redding, Calif., U.S.A.), and then mounted onto the sample stage with double-sided adhesive tabs (Electron Microscopy Sciences) The NSC 11/no Al (MikroMasch, Wilsonville, Oreg., U.S.A.) tip with a resonance frequency of 330 KHz was used. The force constant of the tip was 48 N/m, according to the company, and a scan speed range of 0.5 to 2 Hz was used. All samples were measured in air after drying at ambient temperature.

AFM image analysis

The AFM images were analyzed offline with AFM software (NanoRule+™ 2.0 user's manual 2004). This software can reduce the electronic noise in the raw data to help obtain high-quality images. However, we did not apply any flattening correction to the images so as to retain more of the original structure image information. The bright and dark areas in the images corresponded to peaks and troughs, respectively, of the mass of the gelatin molecules and gel polymers on the mica surface. It should be noted that

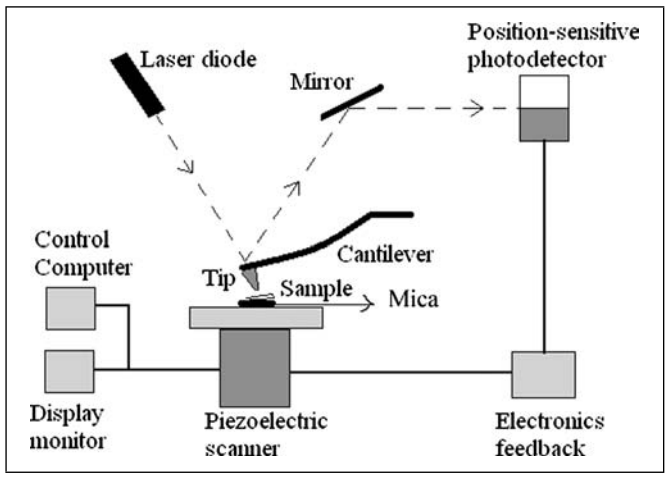

Figure 1—Schematic image of the AFM imaging process (based on Yang and others 2007b)

different scales were used with the vertical and horizontal axes. Images were obtained using both the height mode and the error signal mode. The height mode includes both 3-dimensional and 2-dimensional images. In this mode, the positioning piezo moves the sample so that the tip can respond to the changes in detected force between the sample and the tip and can alter the tip–sample separation distance to restore the force to a predetermined value. This allows a fairly faithful topographical image of the sample to be obtained. The error signal mode removed slow variations in the surface topography but highlighted the edges of the features (http://spm.phy.bris.ac.uk/techniques/AFM/).

The sample dimensions (diameter and height) of the observed aggregates were measured by section analysis, which was done using the AFM software. During the section analysis, the images were analyzed by the software along a line orthogonal to the direction at which the sample images were determined and the surface section profiles were plotted. The characteristic dimensions of the samples were calculated from these surface profiles.

Statistical analysis

Dozens of parallel samples were examined for each specimen to obtain reliable and statistically valid results. Statistical analyses using analysis of variance (ANOVA) ($P < 0.05$) and Duncan's multiple range test for differences in the diameters of the gelatin particles from the AFM images were obtained using SAS software (version 9.1.3; SAS, Cary, N.C., U.S.A.). The data for catfish gelatin were from our experiments and the data for the mammalian gelatin were from the AFM images reported by others (Haugstad and Gladfelter 1994; Lin and others 2002; Saxena and others 2005). The diameters of gelatin particles and annular pores are reported as means ± standard deviations (replicates). Comparisons that yielded P values < 0.05 were considered significant.

Results and Discussion

Screening the imaging parameters

Selecting suitable imaging parameters is important for obtaining high-quality images. There have been several studies using AFM for gelatin imaging (Table 1); however, the gelatins they imaged were almost all from mammalian sources and were analytical or biological grade materials. There were no computer-searchable AFM reports on food-grade gelatin or on gelatins from fish skins. Another problem is that different gelatin samples and imaging techniques require different imaging modes; thus, there is no standard method for examining gelatin samples. In this research, we screened and optimized several important imaging parameters for our samples, including the imaging environment, imaging mode, force constant, and resonance frequency, along with selecting the best cantilever and tip.

Generally, there are 2 environments for AFM imaging, in air and in liquid. The previous reports of AFM imaging of gelatins were done in liquids, including pure water (Radmacher and others 1995), propanol (Radmacher and others 1995, Benmouna and Johannsmann 2004), and butanol (Mackie and others 1998). In water, only the global surface structure is visible with a low resolution at a scale of about 1 μm, while imaging in propanol and butanol could improve the resolution to less than 20 nm (Radmacher and others 1995). For some biological samples, imaging in liquid may give images that are closer to their physiological state. However, the solvent (normally alcohol) may precipitate macromolecules, alter the gel structure, and/or may change the aggregation status of the catfish skin gelatin (Decho 1999; Yang and others 2007b). In order to obtain high-resolution images that, hopefully, closely reflect the original structure of the gelatin, the catfish gelatin was imaged in air.

Imaging mode selection is determined by the sample characteristics and the research's purposes. In general, there are 3 primary imaging modes for AFM operations: contact mode, noncontact mode, and the tapping mode (Yang and others 2007b). The difference between the noncontact mode and the tapping mode is that in the noncontact mode the cantilever is oscillated at a frequency that is slightly above the cantilever's resonance frequency to obtain an AC signal from the cantilever. In the tapping mode the AFM is operated using a tip attached to the end of an oscillating cantilever that intermittently contacts the surface at the lowest point in the oscillation. As we mentioned before, the "noncontact mode" in our AFM is actually a tapping mode according to the definitions normally used for these 3 modes. Gelatin, unlike many other materials previously studied by AFM, is soft and sticky. Therefore, it is very easy to deform and will stick to the tip of the AFM during imaging if unsuitable conditions are applied, giving defective images. Uricanu and others (2003) reported that the same gelatin sample showed different topographical details when imaged with different imaging methods. When imaging samples in air, a large molecular interaction force exists between the sample surface and the tip which, if this interaction could be decreased, would effectively decrease the damage to the sample. Compared with the contact and noncontact modes, the tapping mode reduces the forces between the sample and the tip, along with decreasing the damage to each (Yang and others 2007b). Therefore, the tapping mode was chosen for imaging the gelatin in this research.

After determining the imaging mode and environment, we should select a reasonable force constant and resonance frequency to obtain good images. Generally speaking, the force constant of the tip for tapping mode imaging should be larger than that for contact mode imaging. During tapping mode imaging the tip will easily collapse into the sample if the force constant for the tip is not large enough (http://www.spmtips.com/products/cantilevers/faq/#20). Based on previous experience, and trial and error, it is necessary that the force constant for catfish gelatin be larger than 10 N/m. For frequency selection, since the tapping mode in air is performed by oscillating the cantilever near its resonance frequency, cantilevers with a resonance frequency of 300 kHz and above provide the fastest possible scanning rates. When selecting the cantilever shape, many researchers prefer using a rectangular cantilever rather than a triangular one, because they believe that it is easier to optimize sensitivity (http://www.spmtips.com/products/cantilevers/catalog/tapping/). However, the choice comes down to a personal preference; that is, there are no significant differences in the images with rectangular and triangular cantilevers. A triangular cantilever was preferred for this study since the baseline of the triangular is wider than that of a rectangular cantilever, and it is, therefore, easier to find the tip during sample manipulation.

After determining the cantilever shape and tip force constant, we can select the tips to use. Three types of tips by MikroMasch met our requirements: NSC 11/Ti-Pt, NSC 11/Al BS, and NSC 11/No Al. All 3 tips had 2 triangular cantilevers: A and B. Generally, only 1 cantilever can be used because the other will be destroyed when the tip is mounted on the scanner. For cantilever A, the typical resonance frequency was 75 kHz and typical force constant was 3.0 N/m, while for cantilever B the typical resonance frequency was 330 kHz and the typical force constant was 48 N/m. Cantilever B was selected for imaging the sample. The corresponding cantilever length and width were 90 and 60 μm, respectively. The definitions of the length (l) and width (w) are shown in Figure 2A and the SEM

Table 1—Comparison of the gelatins from different fishes and mammals

Gelatin Source	Reference	Gel strength (bloom)	Type and manufacturer	Imaging parameters	AFM used
Catfish skin	This report	196	Acid after alkaline processed, extracted by authors, Auburn, Ala., U.S.A.	NSC 11/no Al tip, 90 × 60 μm cantilever, 330 kHz resonance frequency, 48 N/m force constant, tapping mode	Nano-R2 (Pacific Nanotechnology Inc., Santa Clara, Calif., U.S.A.
Limed bone	Haugstad and Gladfelter, 1993	—	Type 2688, photographic grade, Kind & Knox Co., Sioux City, Iowa, U.S.A.	Microfabricated 200 μm cantilevers, 0.12 N/m spring constant, pyramidal Si_3N_4 tips	Nanoscope II and III, Digital Instrument Inc., Santa Barbara, Calif., U.S.A.
Limed bone	Haugstad and Gladfelter, 1994	—	Type 2688, photographic grade, Kind & Knox Co.	1231 J scanner, triangular microfabricated 100 μm cantilevers, 0.58 N/m spring constant, pyramidal Si_3N_4 tips	Nanoscope III SFM, Digital Instrument Inc.
Bovine skin	Yao and others 1999	—	Sigma-Aldrich Co., St. Louis, Mo., U.S.A.	Si_3N_4 cantilevers with pyramidal tips, 200 × 12 μm triangular cantilever, 0.12 N/m force constant, contact mode	Nanoscope III, Digital Instrument Inc.
Bovine skin	Saxena and others 2005	75	Type B, Sigma-Aldrich Co.	—	AP 2001, Thermomicroscopes Inc., Sunnyvale, Calif., U.S.A.
Porcine skin	Saxena and others 2005	150 and 300	Type A, Sigma-Aldrich Co.	—	AP 2001, Thermomicroscopes Inc.
Porcine skin	Radmacher and others 1995	—	Sigma-Aldrich Co.	Soft Si_3N_4 cantilevers with integrated pyramidal tips (200 × 12 μm triangular cantilever, prototype cantilevers with oxide sharpened tips, 25 mN/m force constant, contact mode and tapping mode	Nanoscope III, Digital Instrument Inc.
Rat-tail tendon	Usha and others 2004	—	Extracted by authors, Adyar, Chennai, India	180 μm J-scanner, tapping mode, etched silicon probe, single-crystal silicon cantilever	Nanoscope IIIa, Digital Instrument Inc.
Pig	Uricanu and others 2003	—	Type A, Unilever Co., DK, Rotterdam, The Netherlands.	Si_3N_4 tip, 0.1 N/m force constant, contact mode	Home-built Instrument, Postbus, Enschede, The Netherlands.
Pork skin	Benmouna and Johannsmann 2004	175 and 300	Type A, Fluka Co., Heidelberg, Germany.	V-shaped Si_3N_4 cantilevers with 100 μm length, 0.06 N/m spring constant, 10 kHz resonance frequency in water	TMX 2010, TopoMetrix, Inc., Santa Clara, Calif., U.S.A.
—	Lin and others 2002	—	Batch no 2-7157, BASF Co., Ludwigshafen, Germany.	120 μm J-scanner, tapping mode, etched silicon probes, 20 to 100 N/m spring constant, tip and 125 μm cantilever were integrated assembly of single crystal silicon	Nanoscope IIIa, Digital Instrument Inc.
—	Chen and others 1998	—	Ortho-clinical Diagnostics Co., Ascot, Berkshire, U.K.	E-type scanner, TESP silicon tips with rectangular cantilever of 125 μm long, 50 N/m force constant, 300 kHz resonance frequency, tapping mode	Nanoscope IIIa, Digital Instrument Inc.
—	Mackie and others 1998	300	Gelatine Products Co., Runcorn, Cheshire, U.K.	Nanoprobe Si_3N_4 cantilevers, 0.38 N/m force constant, imaged in liquid cell, *dc* constant force mode	East Coast Scientific Inc., Cambridge, U.K.
—	Mohanty and Bohidar 2005	—	Type B, E. Merck Co., Ltd, Worli, Mumbai, India.	90 μm scanner, noncontact mode	AP 2001, Thermomicroscopes Inc.

Gelatin type A is derived from acid-processed collagen, type B is obtained from alkaline-processed collagen.

image of the shorter cantilever of the NSC 11 series is shown in Figure 2B. After trial and error using these 3 tips, the NSC 11/No Al tip was found to be the most suitable for fish gelatin as it gave more stable images.

Nanostructural characterization of catfish skin gelatin

Gelatin is the denatured form of collagen, which is originally a triple helix with 3 single α-helices wrapped around each other. During denaturation, the collagen molecule is broken into smaller pieces and the triple helices become single helices with molecular weights ranging between 20 and 100 kDa depending on preparation and raw material source (Radmacher and others 1995). Higher molecular weights are usually characteristic of better preparations.

AFM can create 3-dimensional images with resolution down to the nanometer scale, which has made it an essential tool for applications requiring imaging surfaces. Height mode imaging data are 3-dimensional and a color mapping for height is used to display the data (dark for low features and bright for high features). In addition to this height mode, the error-signal mode images can

provide high-contrast images of the same objects. Similar color mappings of the data can also be used for this imaging mode (http://spm.phy.bris.ac.uk/techniques/AFM/).

Our work focused on the self-association of gelatin using AFM. Nanoscale structural information of gelatin molecules and their aggregates can be obtained from AFM images of both height and error-signal modes (Saxena and others 2005). All of the surface images are roughly in the nanoscale range and show that the mica surface is completely covered with the gelatin. Thus, all the structural information obtained from the AFM images is characteristic of the gelatin applied to the mica. The coiled conformation of catfish skin gelatin in aqueous solution can be seen from the AFM height mode images (Haugstad and Gladfelter 1994).

Figure 3 shows the typical spherical structure of the gelatin. The height mode (including 2- and 3-dimensional images) and the error-signal mode AFM images of catfish skin gelatin can be obtained simultaneously. It should be noted that both the horizontal and vertical scales of the images are irregular because they are produced by the machine directly. Most of the fish gelatin samples showed the expected spherical structure with different diameters (for example, W1, W2 in Figure 3). The average diameter of these spherical structures was 267 ± 131 nm ($n = 51$) ranging from 89.9 to 820.4 nm. Occasionally, cavity structures attributed to swelling of the gelatin were also found in some AFM images (as shown in Figure 4). In these swelling cavity structures annular pores were observed. The average diameter of these annular pores was 118 ± 14 nm ($n = 3$). The size of these pores is a little larger than that obtained from a mammalian-grade photographic gelatin (Haugstad and Gladfelter 1993). The annular pores of the previously studied limed bone gelatin film had diameters of about 10 to 100 nm. This gelatin had been deposited on highly oriented pyrolytic graphite (Haugstad and Gladfelter 1993). It seems that more water was aggregated with this fish gelatin than that mammalian gelatin based on the larger pore size.

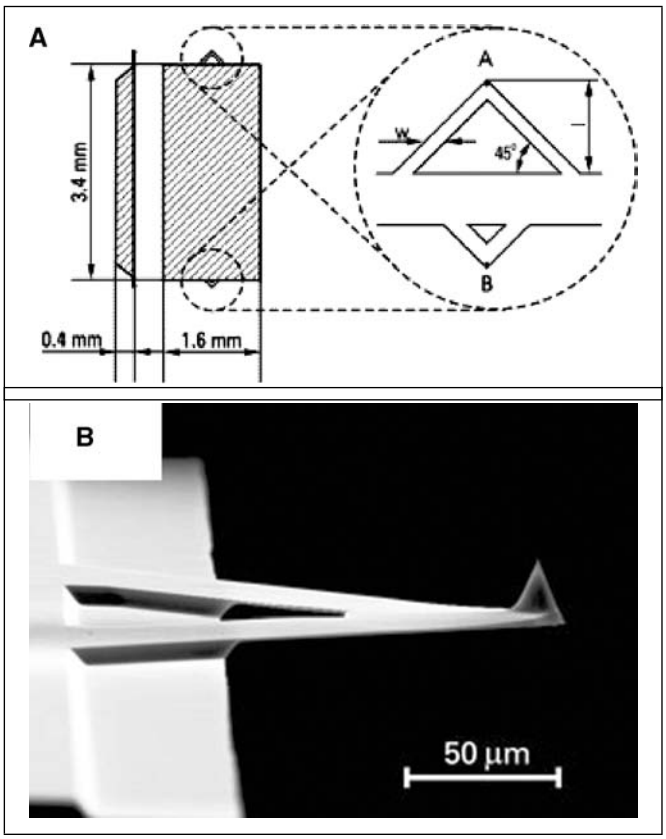

Figure 2—Schematic image using a triangular cantilever and a tip for AFM imaging. (A) The silicon chip of the NSC11 series tips has 2 triangular cantilevers. The thickness of the chip is 0.4 mm, *l* and *w* denote the length and width of the cantilever, respectively. (B) SEM image of the shorter cantilever chip of the NSC11 series (available from: http://www.spmtips.com/nsc11/noal).

The range of aggregate diameters of the catfish gelatin suggests that the gelatin, as expected, is a heterogeneous structure (Figure 5A, 5B). The initial concentration of gelatin for AFM imaging is very low and then air-dried at room temperature. It can be assumed that the gelatin gel film formed on the mica surface can still be assumed to be at low concentrations, which suggests that gelatin molecules can aggregate even if the solution is too diluted to form a gel (Ward and Courts 1977).

Both the AFM height mode and error-signal mode images can show the association of catfish skin gelatin. AFM images of gelatins incubated for different time periods were compared to illustrate the association process. The AFM images of these samples after being freshly diluted are shown in Figure 5A, 5B, and AFM images of samples that were incubated in air at room temperature for 1 h are shown in Figure 5C to 5F. This comparison clearly shows that both the fibril structure and the spherical coil structure existed during the aggregation period. The AFM images of these samples after incubation are different from the commonly observed spherical structure of the AFM images that are deposited directly onto the mica surface without incubation (Figure 5A, 5B), suggesting that both multimers and monomers might participate in the association of the gelatin molecules. Figure 5C to 5F directly show the visible fibril structure of gelatin, which is similar to the results of Uricanu and others (2003) and Lin and others (2002). Lin and others (2002) proposed that the aggregation of gelatin molecules occurred mainly by a multimeric association process in which multimers aggregated to form cluster structures that then associated further. Furthermore, they suggested that the aggregates are stabilized by ionic interactions between oppositely charged units, hydrogen bonds, and hydrophobic interactions.

It should be noted that most of the previous reports about gelatin using AFM were performed in liquids (Radmacher and others 1995; Mackie and others 1998; Benmouna and Johannsmann 2004). Even though the forces between the tip and the samples can be reduced by imaging in liquid, thus minimizing destruction of the original surface structure, the butanol and other alcohols used as the liquid media for imaging will influence the structure of the gelatin, as was previously mentioned. Generally, gelatin will shrink in these liquids. In this study, the samples were imaged in air and the gelatin structures from the AFM images were, we believe, closer to that which would be produced when these gelatins are used commercially as we believe the air-drying of the dilute solution will lead to fewer artifacts.

Based on the experiments, we propose the following 2 pathways for the aggregation of fish gelatin during hydrolysis and sample drying (Figure 6). Both of these pathways have 3 major steps. In the 1st step, during sodium hydroxide and acetic acid treatment, the ions penetrate the collagen and form gelatin molecules; that is, the ionized solutions lead to the breakdown of the collagen. In the 2nd step, aggregation interactions occur between the gelatin molecules, between gelatin molecules and water molecules, and between gelatin molecules and the added ions. In the last step, the water molecules are evaporated by drying prior to AFM imaging. These are the aggregates of the catfish gelatin that were obtained and imaged by AFM. However, the details of the 3 steps in the 2 pathways being proposed are slightly different. For pathway

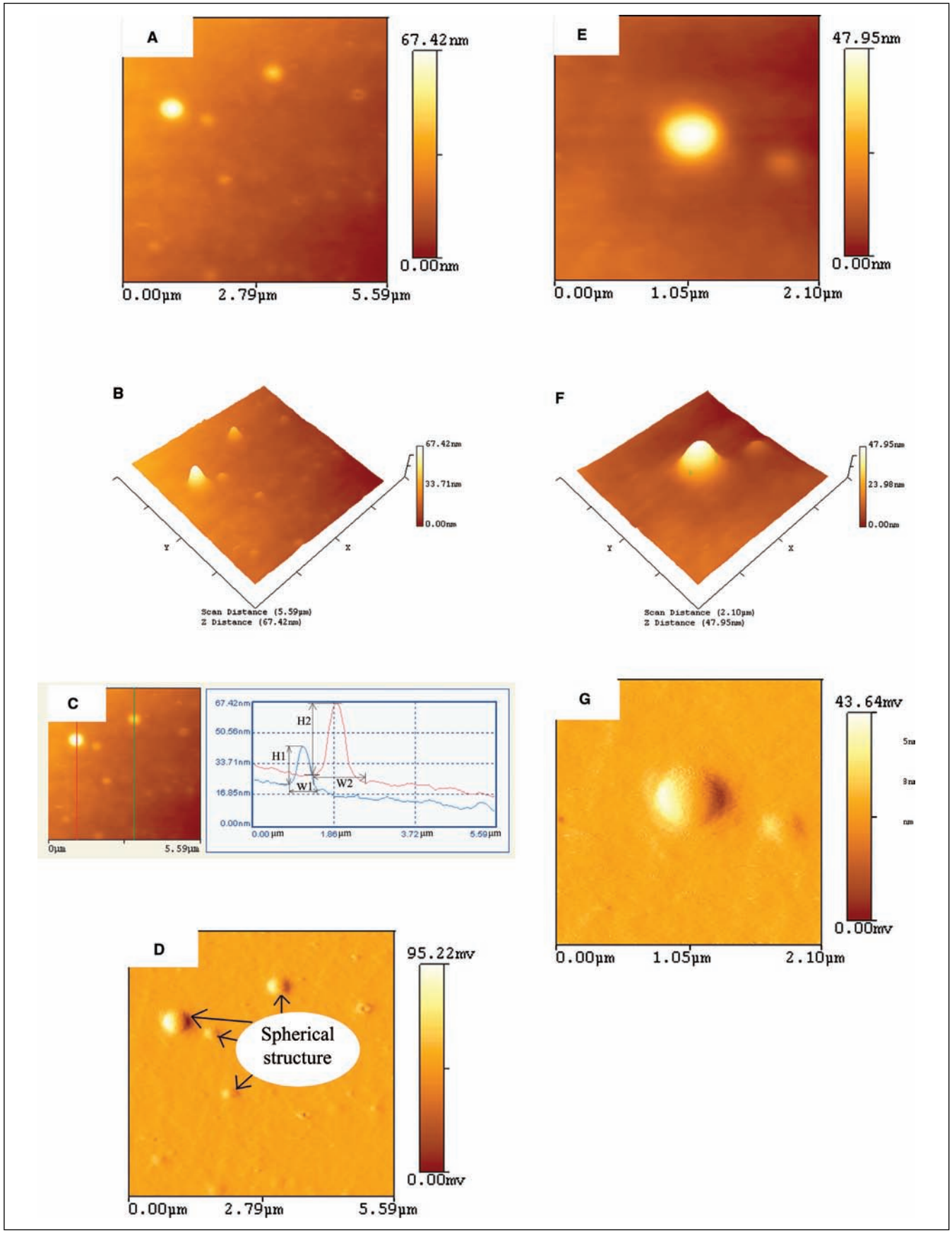

Figure 3 — Typical AFM images of catfish skin gelatin. (A) 2-dimensional height mode image; (B) 3–dimensional version of the corresponding 2-dimensional height mode image; (C) dimensions of the nanoparticles, *H* means the height and *W* means the diameter of the corresponding particles; (D) error signal mode image; (E) enlarged plane height mode image; (F) enlarged 3-dimensional height mode image; (G) enlarged error signal mode image.

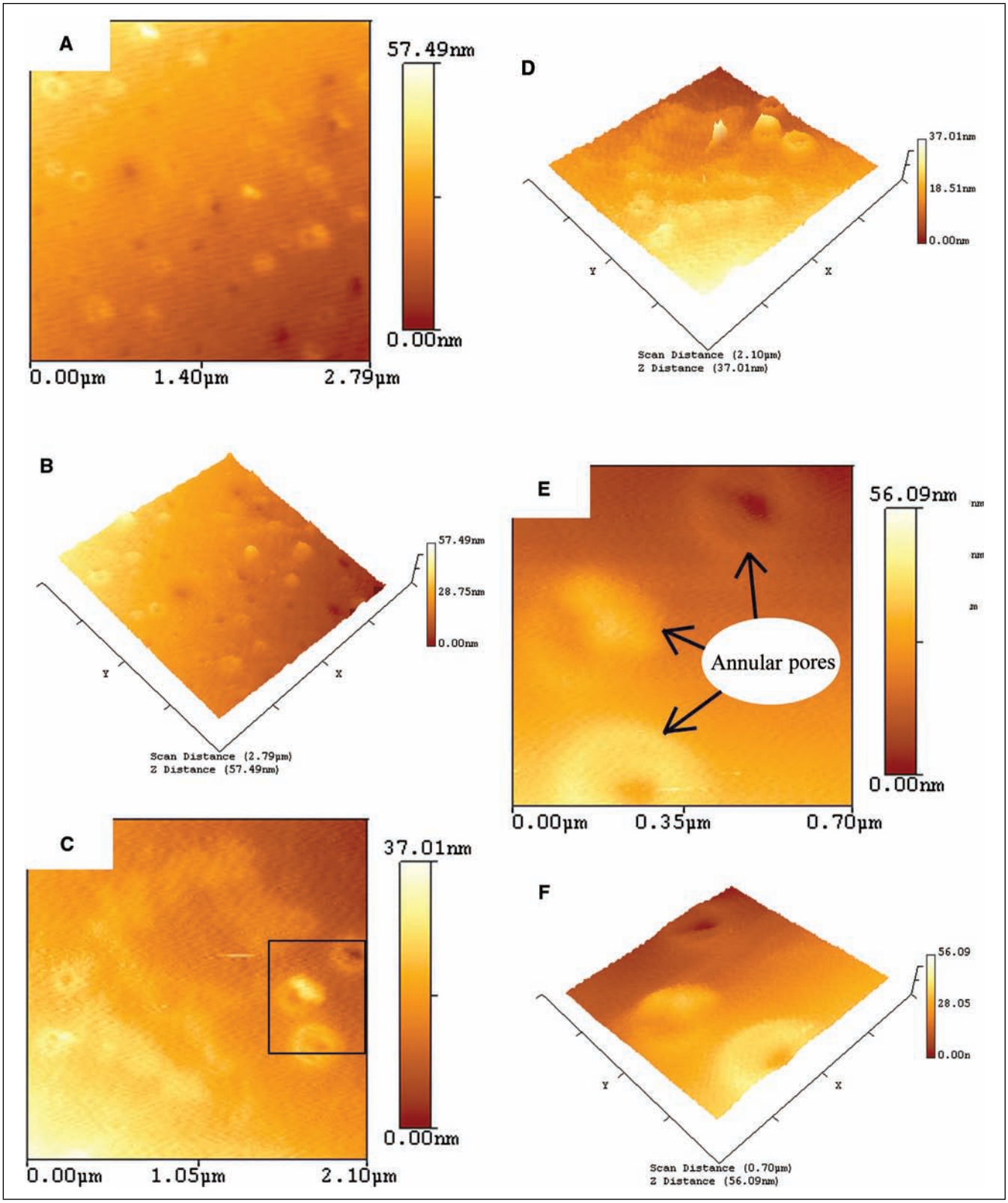

Figure 4—AFM images of the swelling cavity structure of catfish skin gelatin. (A) plane image of general material; (B) corresponding 3-dimensional image; (C) plane image of a selected part; (D) corresponding 3-dimensional image; (E) enlarged plane image of c; (F) corresponding 3-dimensional image.

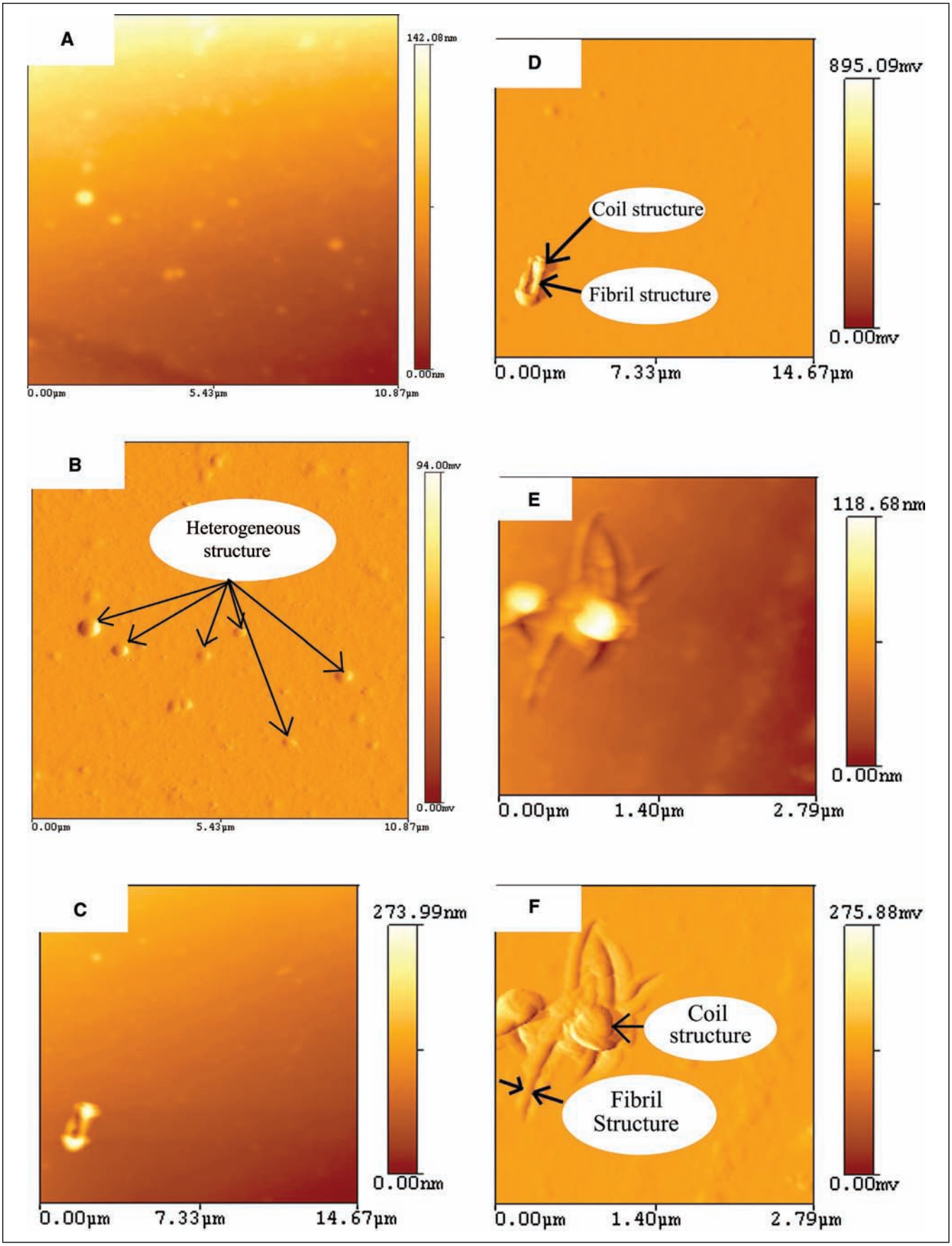

Figure 5—Effects of time on macromolecular aggregation of catfish skin gelatin. (A) plane height mode image; (B) error signal mode image; (C) plane height mode image of sample incubated for 1 h; (D) error signal mode image of the same material; (E) another plane height mode image of sample incubated for 1 h; (F) error signal mode image.

1, a large amount of water with salt ions penetrates into the gelatin molecules during hydrolysis and aggregation, then more gelatin molecules conglomerate at the outer layer of the water aggregates during aggregation; thus, a large water pool is formed with a spherical shape. The water in this pool is evaporated during the air-drying before AFM imaging and is then observed as a hollow structure surrounded by gelatin. There are no observed effects of the remaining salt since it can be considered negligible in both amount and size, that is, after water evaporation the annular pores are left in the central part of the gelatin aggregates, as shown in Figure 4. In pathway 2, the solution penetrated into the gelatin molecules with minimal aggregation. Therefore, although many small water droplets and ions penetrated into the gelatin molecules, they are separated from one another by gelatin molecules. Thus, the result of the hydrolysis is a more even distribution and aggregation of water and salt ions. Then only small water pools are formed in the process. The encompassing gelatin molecules are more inclined to join together during the water evaporation before AFM imaging, leading in the end to formation of compact spheres (as shown in Figure 3). Our previous research showed that alkali treatment has a significant effect on the swelling characteristics of collagen (Yang and others 2007a). At the same pH value, sodium hydroxide led to greater swelling than lime. Electron microscopy showed that there was some loss of structure of the collagen fibers after sodium hydroxide treatment, leading eventually to complete separation of the fibrils. This degradation of collagen was not observed with either lime or sodium sulfate solutions (Johns and Courts 1977). Thus, it can be assumed that the hydrolysis of collagen was more uniform with the sodium hydroxide solution. This hypothesis was supported by the typical structures seen in Figure 3 and those structures only occasionally seen in Figure 4.

The data obtained with AFM do have some limitations. Probe-broadening effects and side-by-side association of molecules are 2 common factors that contribute to data imprecision (Yang and others 2006b). The geometrical effect can be estimated by calculating the deviation in radius (r) of a cylindrical molecule of measured width (w) that is broadened by a tip of radius (R), using the relationship $r = w^2/16R$ (Morris and others 1997; Yang and others 2006b). In Figure 5, suppose the width of the linear gelatin molecule is 30 nm and the typical tip curvature radius of the NSC 11/No Al tip is about 10 nm; then the deviation of the radius (r) is about 5.6 nm.

Saxena and others (2005) believed that the nanoparticles of gelatin biopolymers were formed mainly through both inter- and intramolecular electrostatic interactions. In the beginning of nanoparticle formation, there is a competition between intramolecular folding and intermolecular aggregate formation. Two charged segments join together through electrostatic attraction, if and only if these come within a distance that is less than the Debye–Huckel screening length. In the end, such nanoparticles would be spherical.

These results will help us to further understand the self-aggregation mechanisms of the gelatin molecules at a nanoscale, and they provide a new way to investigate the structure–property-function relationships of gelatin (Lin and others 2002).

Comparison of the nanostructure and physical property of fish gelatin with those from other gelatin sources

Figure 7 shows the frequency histogram for the different diameters of catfish skin gelatin particles obtained from AFM images. From Figure 7, it can be seen that most of the diameter values are in the range of 160 to 280 nm.

Table 2 shows the comparison of the diameters of gelatin particles and the gel strength of gelatins from different sources. The experimental results show that the average diameters of catfish skin gelatin aggregates formed are 267 ± 131 nm (n = 51), as discussed earlier, which is consistent with the common observation of the range for gelatin nanoparticles from bovine skin and porcine skin, where the average diameter is 180 ± 42 nm (Saxena and others 2005). The diameters of these spherical aggregates by AFM are comparable to those obtained by traditional methods, including osmotic pressure, viscosity, light scattering, flow birefringence, and sedimentation methods. With these traditional methods, gelatin molecules are generally thought to be about 150 nm in diameter (Ward and Courts 1977). AFM is more direct and easier to use to obtain the diameter compared to traditional methods. Few previous publications mentioned both the size of the aggregates and the gel strength in the same report. Only the diameters of the nanoparticles, as well as bloom value of type A (which is prepared by an acid process) porcine skin, have been reported (Saxena and others 2005). Our results showed that the diameters of the nanoparticles of catfish gelatin are larger than that of a type A porcine skin, while the bloom value is lower than the latter. The bloom values of the type B No. 2-7157 and type 2688 gelatins reported by Lin and others (2002) and Haugstad and Gladfelter (1993, 1994) are not available. Type B means that the gelatin was prepared by an alkaline process. The average diameter of the nanoparticles of

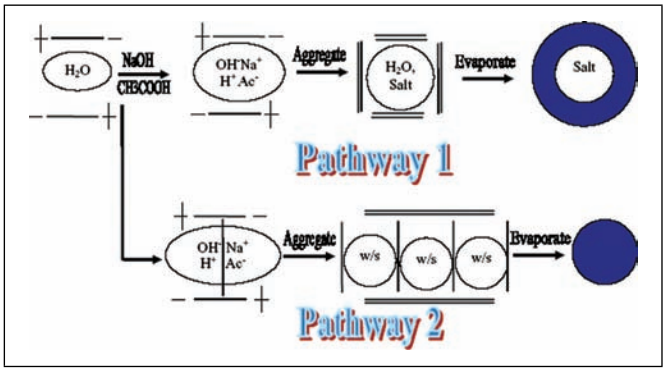

Figure 6—Hypothetical schematic images of the catfish skin gelatin aggregates formed. Note: "w" denotes water with ion or salt; "s" means salt; "Ac⁻" means the anion of acetic acid; "+ — −" means amphiphatic structure of gelatin molecule.

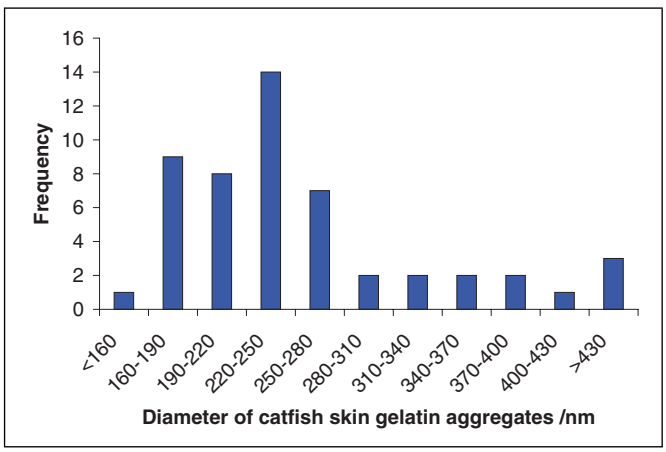

Figure 7—Frequency histogram for the diameters of catfish skin gelatin aggregates. Note: The number of nanoparticles is 51. The average diameter was 267 ± 131 nm.

Table 2—Comparison of the diameters of different gelatin nanoparticles

Gelatin	Diameter of nanoparticles (nm)	Bloom (g)
Acid after alkaline-processed catfish skin	267 ± 131 (51)[b]	196 ± 5 (5)
Type A porcine skin, Sigma-Aldrich Co., St. Louis, Mo., U.S.A.	180 ± 42 (20)[c]	300
Type B No. 2-7157, BASF, Ludwigshafen, Germany	32.3 ± 10.4 (70)[d]	—
Type 2688, photographic grade, from limed bone, Kind & Knox Co., Sioux City, Iowa, U.S.A.	889 ± 182 (8)[a]	—

Data other than catfish skin were obtained from the AFM results in Saxena and others (2005), Lin and others (2002), and Haugstad and Gladfelter (1994).
The data are reported as means ± standard deviations (replicates) where applicable.
Values in the same column with different superscript letters indicate significant differences by the Duncan's multiple range test ($P < 0.05$).

type 2688 gelatin (890 nm) is much larger than that of catfish gelatin (267 nm), while the values of type A porcine skin and type B sample No. 2-7157 are smaller than that of catfish gelatin. Further research should be conducted with additional gelatins to determine an in-depth relationship between nanostructure and gel strength.

It should be noted that our preparation procedures for the fish gelatin for AFM are very different from that reported by Saxena and others (2005) who used a 2-step desolvation method.

Gelatin is an amphoteric polyelectrolyte (polyampholyte) containing both positively and negatively charged monomers within the molecule (Lin and others 2002). Thus, pH is a possible factor influencing the aggregation of the gelatin. Lin and others (2002) observed the gelatin molecules collapse at the isoelectric point of a mammalian gelatin (Type B No. 2-7157; BASF, Ludwigshafen, Germany), and they believed the phenomenon due to the electrostatic attraction forces of oppositely charged groups, and, in turn, an intermolecular association process takes place and results in self-association. The soluble aggregates are thought to be stabilized by ionic contacts, hydrogen bonds, and hydrophobic interactions, and are free of participation by hydrophilic groups on the surface of the particles. For pH values away from the isoelectric point, the gelatin molecular chains behave more like random coils, and the association–disassociation is based mainly on electrostatic interactions that are reversible to a certain degree. However, the sizes of the particles formed are stable with a change of pH. Furthermore, for a certain gelatin, the sizes of the particles formed are also stable and do not change much with temperature and the molecular weight of the polypeptide (Saxena and others 2005). Thus, the diameters of different gelatins can be compared without considering the pH and temperature of these gelatin aggregates (Saxena and others 2005). Therefore, the diameters of the catfish gelatin can be compared with the gelatins from other sources, even though the conditions of pH and temperature were not the same.

AFM imaging in liquids showed that at the low levels of helical content, which were found in the mammalian gelatin molecules, they assemble into aggregates containing short segments with lengths and diameters comparable to those expected for gelatin triple helices. Larger fibrous structures appeared whose sizes indicated that they were bundles of triple helices, increasing with time. During gelation, the number density of the fibers increased at the expense of the smaller aggregates. These fibers then eventually associated into a fibrous network (Mackie and others 1998). Mohanty and Bohidar (2005) found that the coacervate phase of mammalian gelatin is a relatively 2-dimensional, dense, heterogeneous material comprising strongly interconnected triple helices, which imparts a large storage modulus (G') to this material. Further molecular manipulation of the fish gelatin before AFM imaging should be conducted to investigate the characteristics of the fibrous structures of fish gelatin (Yang and others 2006a).

Conclusions

The nanostructure of catfish (*Ictalurus punctatus*) skin gelatin was successfully imaged by AFM. The gelatin was extracted with the optimized process previously developed. The AFM images show that most of the aggregates are spherical structures with an average diameter of 267 ± 131 nm; and annular pores can occasionally be obtained with an average diameter of 118 ± 14 nm. With incubation in air at room temperature for 1 h before imaging, the AFM images showed an aggregation process, which originated from the small coiled molecules associating with the linear structures to form larger coil aggregates. Height mode and error signal mode images can be obtained simultaneously. We also proposed a theory to explain the different structures formed. The results indicate that AFM is a powerful tool to obtain integrated and direct information on the structure and properties of gelatin macromolecules and aggregates.

Acknowledgments

This research was supported by the Alabama Agricultural Land Grant Alliance (AALGA) and the Alabama Agricultural Experiment Station (AAES). Project 30600420 supported by National Natural Science Foundation of China also contributed to this research. The authors thank Harvest Select Inc. (Uniontown, Ala., U.S.A.) for the donation of catfish skin and Harvey J. Pine for delivering the samples. We thank Dr. Christine W. Curtis, Dr. William R. Ashurst, Adam Anderson, and Aimee Poda from the Dept. of Chemical Engineering at Auburn Univ. for assistance in performing the AFM experiments.

References

Badii F, Howell NK. 2006. Fish gelatin: structure, gelling properties and interaction with egg albumen proteins. Food Hydrocolloids 20:630–40.
Benmouna F, Johannsmann D. 2004. Viscoelasticity of gelatin surfaces probed by AFM noise analysis. Langmuir 20:188–93.
Chen X, Davies MC, Roberts CJ, Tendler SJB, Williams PM, Davies J, Dawkes AC, Edwards JC. 1998. Interpretation of tapping mode atomic force microscopy data using amplitude-phase-distance measurements. Ultramicroscopy 75:171–81.
Cho SH, Jahncke ML, Chin KB, Eun JB. 2006. The effect of processing conditions on the properties of gelatin from skate (*Raja kenojei*) skins. Food Hydrocolloids 20:810–6.
Choi SS, Regenstein JM. 2000. Physicochemical and sensory characteristics of fish gelatin. J Food Sci 65:194–9.
Decho AW. 1999. Imaging an alginate polymer gel matrix using atomic force microscopy. Carbohydr Res 315:330–3.
DiOrio JP, Stojanovic L, Yardimci A, Amrani DL, Helgerson S, Vega F. 2005. Electron microscopic characterization of a gelatin matrix/thrombin hemostat. Microsc Microanal 11(S2):178–9.
Foegeding EA. 2006. Food biophysics of protein gels: a challenge of nano and macroscopic proportions. Food Biophys 1:41–50.
Gómez-Guillén MC, Turnay J, Fernández-Díaz MD, Ulmo N, Lizarbe MA, Montero P. 2002. Structural and physical properties of gelatin extracted from different marine species: a comparative study. Food Hydrocolloids 16:25–34.
Haugstad G, Gladfelter WL. 1993. Atomic force microscopy of AgBr crystals and adsorbed gelatin films. Langmuir 9:1594–600.
Haugstad G, Gladfelter WL. 1994. Probing biopolymers with scanning force methods: adsorption, structure, properties, and transformation of gelatin on mica. Langmuir 10:4295–306.
Ikeda S. 2003. Heat-induced gelation of whey proteins observed by rheology, atomic force microscopy, and Raman scattering spectroscopy. Food Hydrocolloids 17:399–406.
Ikeda S, Morris VJ. 2002. Fine-stranded and particulated aggregates of heat-denatured whey proteins visualized by atomic force microscopy. Biomacromolecules 3:382–9.
Jamilah B, Harvinder KG. 2002. Properties of gelatins from skins of fish—black tilapia (*Oreochromis mossambicus*) and red tilapia (*Oreochromis nilotica*). Food Chem 77:81–4.

Johns P, Courts A. 1977. Relationship between collagen and gelatin. In: Ward AG, Courts A, editors. The science and technology of gelatin. New York: Acdemic Press. p 164–5.
Lin W, Yan Y, Mu C, Li W, Zhang M, Zhu Q. 2002. Effect of pH on gelatin self-association investigated by laser light scattering and atomic force microscopy. Polym Int 51:233–8.
Mackie AR, Gunning AP, Ridout MJ, Morris VJ. 1998. Gelation of gelatin observation in the bulk and at the air–water interface. Biopolymers 46:245–52.
Mohanty B, Bohidar HB. 2005. Microscopic structure of gelatin coacervates. Int J Biol Macromol 36:39–46.
Morris VJ, Gunning AP, Kirby AR, Round A, Waldron RK, Ng A. 1997. Atomic force microscopy of plant cell walls, plant cell wall polysaccharides and gels. Int J Biol Macromol 21:61–6.
NanoRule^{+TM} 2.0 user's manual. 2004. Santa Clara, Calif., U.S.A.: Pacific Nanotechnology Inc.
Radmacher M, Fritz M, Hansma PK. 1995. Imaging soft samples with the atomic force microscope: gelatin in water and propanol. Biophys J 69:264–70.
Saxena A, Sachin K, Bohidar HB, Verma AK. 2005. Effect of molecular weight heterogeneity on drug encapsulation efficiency of gelatin nano-particles. Colloid Surf B-Biointerfaces 45:42–8.
Uricanu VI, Duits MHG, Nelissen RMF, Bennink ML, Mellema J. 2003. Local structure and elasticity of soft gelatin gels studied with atomic force microscopy. Langmuir 19:8182–94.
Usha R, Dhathathreyan A, Mandal AB, Ramasami T. 2004. Behavior of collagen films in presence of structure modifiers at solid-liquid interface. J Polym Sci 42:3859–65.
Vardhanabhuti B, Ikeda S. 2006. Isolation and characterization of hydrocolloids from monoi (*Cissampelos pareira*) leaves. Food Hydrocolloids 20:885–91.
Wainewright FW. 1977. Physical tests for gelatin and gelatin products. In: Ward AG, Courts A, editors. The science and technology of gelatin. New York: Acdemic Press. p 507–21.
Ward AG, Courts A. 1977. The science and technology of gelatin. New York: Academic Press.
Yang H, An H, Li Y. 2006a. Manipulate and stretch single pectin molecules with modified molecular combing and fluid fixation techniques. Eur Food Res Technol 223:78–82.
Yang H, Lai S, An H, Li Y. 2006b. Atomic force microscopy study of the ultrastructural changes of chelate-soluble pectin in peaches under controlled atmosphere storage. Postharvest Biol Technol 39:75–83.
Yang H, Wang Y, Jiang M, Oh JH, Herring J, Zhou P. 2007a. Two-step optimization of the extraction and subsequent physical properties of channel catfish (*Ictalurus punctatus*) skin gelatin. J Food Sci 72:C188–95.
Yang H, Wang Y, Lai S, An H, Li Y, Chen F. 2007b. Application of atomic force microscopy as a nanotechnology tool in food science. J Food Sci 72:R65–75.
Yao K, Liu W, Lin Z, Qiu X. 1999. In situ atomic force microscopy measurement of the dynamic variation in the elastic modulus of swollen chitosan/gelatin hybrid polymer network gels in media of different pH. Polym Int 48: 794–8.
Yoshimura K, Terashima M, Hozan D, Shirai K. 2000. Preparation and dynamic viscoelasticity characterization of alkali-solubilized collagen from shark skin. J Agric Food Chem 48:685–90.
Zhou P, Mulvaney SJ, Regenstein JM. 2006. Properties of Alaska pollock skin gelatin: a comparison with tilapia and pork skin gelatins. J Food Sci 71:C313–21.